JEE Journal of Ecological Engineering

Journal of Ecological Engineering, 2026, 27(9), 353–365
https://doi.org/10.12911/22998993/222387
ISSN 2299–8993, License CC-BY 4.0

Received: 2026.03.22
Accepted: 2026.07.15
Published: 2026.08.01

Sustainable removal of phenol from polluted wastewater using phosphoric acid activated biochar prepared from date kernels

Marwan Arkan Hussein[1*], Sarah Asif Abdullah[1],
Nadia Matter Almhana[1], Manar Banwan Hasan[1]

[1] Department of Environmental Engineering, College of Engineering, Al-Mustansiriyah University, Baghdad, Iraq
* Corresponding author's e-mail: marwana.hussein@uomustansiriyah.edu.iq

ABSTRACT

Phenolic compounds are among the most hazardous organic pollutants commonly detected in industrial wastewater due to their toxicity, persistence, and resistance to biodegradation. In this study, phosphoric acid-activated biochar derived from date kernels (DK) was synthesized as a sustainable and low-cost adsorbent for phenol removal from aqueous solutions and real refinery wastewater. The activation process significantly enhanced the physicochemical properties of the biochar, increasing the BET surface area from 2.11 to 1087 m^2/g and the pore volume from 0.0031 to 0.818 cm^3/g. The prepared adsorbent was characterized using FTIR, SEM, BET, and XRD analyses. Batch adsorption experiments were conducted under different operational conditions, including pH (3–11), contact time (30–150 min), adsorbent dosage (0.4–1.2 g), initial phenol concentration (50–250 mg/L), and agitation speed (100–250 rpm). The optimum adsorption conditions were achieved at pH 5, contact time of 120 min, adsorbent dosage of 0.8 g, initial phenol concentration of 50 mg/L, and agitation speed of 200 rpm, resulting in a phenol removal efficiency exceeding 99%. Adsorption equilibrium data were best described by the Langmuir isotherm model (R^2 = 0.9943), indicating predominantly monolayer adsorption, while kinetic analysis showed the best fit with the pseudo-second-order model (R^2 = 0.999). The Dubinin–Radushkevich model suggested that physical adsorption interactions also contributed to the overall adsorption mechanism. Application of the developed adsorbent to real refinery wastewater reduced phenol concentration from 10.65 to 1.11 mg/L with a removal efficiency of 89.58% and the adsorption capacity is 62 mg/g. The findings demonstrate that phosphoric acid-activated date kernel biochar is a promising, eco-friendly adsorbent for efficient phenol removal from wastewater.

Keyword: date kernels, phenol, activated biochar, acid, wastewater, removal by adsorption.

INTRODUCTION

The rapid growth of industrialization, a growing population, and the urban environment attribute for increasing of produced wastewater globally (Nasir et al., 2022; Önal and Küçük, 2020). Due to this, the water resources face a lot of pressure, since the untreated or poorly treated wastewater can enter the rivers, lakes and groundwater, causing, in the long term, damage to the environment (Chen et al., 2022). Not only does wastewater increase the demand on clean water supplies, but the mixture of pollutants within wastewater presents serious threats to public health and ecology (Kariem et al., 2018; Manasa and Mehta, 2020).

Industrial and municipal wastewaters are known for their complex composition, which incorporates a wide variety of pollutants, including heavy metals, synthetic dyes, pharmaceuticals, pesticides, hydrocarbons, and other organic and inorganic compounds. The removal of many of these contaminants poses a continuous environmental science and engineering challenge; they are toxic, non-biodegradable, and resistant to traditional treatment processes (Hussain et al., 2023).

Phenolic compounds are one of the types of pollutants that have attracted significant concerns due to their toxic effect at low concentrations. Phenolic compounds are extensively discharged into wastewater by the effluents from

petrochemical, pharmaceutical, plastic, resin dyeing, and paper industries. They are highly soluble in water and resist biodegradation, thus persisting in aquatic systems, where they may produce carcinogenic, mutagenic and teratogenic effects on humans and also lethally affect aquatic organisms (Al-Khalid et al., 2020). Phenols are priority pollutants defined by the U.S. Environmental Protection Agency (EPA) and the World Health Organization (WHO), and their removal is increasingly urgent (Farzana et al., 2023).

Conventional treatment technologies have many drawbacks, such as high cost, incomplete dosage, and generation of secondary toxic products by means of chemical oxidation, organic degradation, membrane separation, etc. (Nhat-Thien Nguyen et al., 2025). On the other hand, adsorption is widely accepted as one of the optimal and economic methodologies for phenolic compounds elimination because of its simple process, materials reusability, and high efficiency removal rate (El-Naas et al., 2010).

In recent years, there has been increasing interest in the application of eco-friendly, low-cost, and sustainable adsorbents from agricultural by-products (Alfyad et al., 2025; Saravanan et al., 2021). Date seeds (date pits), commonly found in date-producing districts, are a potential candidate for this purpose (Bartolomeu et al., 2018). They are discarded, because they belong to a high agro-waste category of the date palm industry, even though they serve carbon-rich and plethora porous structures that can be improved through activation methods (Abdullah et al., 2025; Hualpa-Cutipa et al., 2022). The use of date pits as the adsorbent can not only offer a cost-effective, green method for phenol elimination, but also promote environmental sustainability through waste valorization and resource recovery (Kumar et al., 2021).

While the phenol adsorption performance of biochar and activated carbon has previously been studied, few studies focused on phosphoric acid-activated biochar obtained from detailed characterization of date kernels, followed by application to real refinery wastewater. In addition, most previous works focus only on removal efficiency, while the relationship between adsorption performance and surface structural evolution, as well as adsorption mechanism and kinetic behavior are still not well correlated. Therefore, this study aimed to prepare and characterize phosphoric acid-activated date kernel biochar and evaluate its performance for phenol removal under different operational conditions using both synthetic and real industrial wastewater samples.

MATERIAL AND METHODS

Collection and preparation of Date Kernel

The collected kernel was washed with filtered water to remove dust and other unknown contaminants (Figure 1a). It was then heated to 105 °C for 24 hours in a hot oven, ground into a smooth powder in a grinding machine, and sieved to particles smaller than 1 mm (Mohamad Said et al., 2021) to prepare the adsorbents before the activation process (Figure 1b).

(a) DK after cleaning (b) DK after grinding

Figure 1. Step preparation DK before activation process

Chemical activation process

Although it effectively improves the adsorptive capacity of the activated biochar (ABC) for a range of pollutants, especially phenolic substances, phosphoric acid activation of activated biochar has garnered a lot of attention. Phosphoric acid functions as a dehydrating agent to facilitate the formation of a porous architecture inside the matrix of carbon obtained from agricultural waste, including nut shells, which ultimately improves the surface area and porosity. Since more surface area typically translates into more active sites accessible for adsorption, this feature is crucial (Yang et al., 2021).

According to Hussain (Hussain et al., 2023), phosphoric acid (H_3PO_4) was used in the DK chemical activation process to create activated biochar. In short, 100.0 g of crushed DK were steeped in the acid phosphoric at a ratio of 1:3 (w/w). The mixture was gently agitated, heated to 70 °C for two hours, and subsequently allowed to rest at ambient temperature overnight to ensure thorough absorption of the acid. The mixture was subsequently positioned in a muffle furnace, which was heated up to 500.0 °C for 2 hours, at a constant rate of 5 °C per minute. The water that was distilled was used for the removal of acidic chemicals till the pH reached 6.8; subsequently, a conventional electric oven was utilized to dry the activated charcoal for 24 hours at 105.0 °C. Therefore, following activation, the material was ready, as seen in Figure 2.

Figure 2. Preparation of DK after activation process

Preparation of stock solutions

The tests on the ad were conducted using a 1000 ppm phenol stock solution to eliminate other impurities or elements that could affect accuracy, as well as the quality of the results. One gram of phenol was dissolved in one liter of distilled water (Alhamd et al., 2024). An equal volume of ethanol was added to the filtered succinic acid, and gently mixed at room temperature for 15 mins.

Batch experiments

To determine the effect of different factors on phenol elimination, several experiments were carried out in a batch system. Each experiment involved filling a 250 mL semicircular flask with 200 mL of distilled water and an adsorbate solute at different concentrations. The flask was then placed in an orbital shaker with different experimental settings. The samples were filtered at predetermined intervals using a manual sieve. The concentration of an aqueous solution in the test samples was then ascertained using a spectrophotometer. The equilibrium amount of phenol adsorbed onto DK was estimated using the formula below: Equations 1 and 2 for removal efficiency percentage and the adsorption capacity. Table 1 lists parameters used in these experiments.

$$q_e = \frac{(C_0 - C_e)V}{W} \quad (1)$$

$$Removal\ percentage = \frac{C_o - C_e}{C_o} \times 100 \quad (2)$$

where: *Co* and *Ce* are the concentrations of solution contaminants at the starting and equilibrium states (mg/L), respectively, the steady state pollutant uptake is reflected in DK (mg/g) via *qe*, *V* – Provides the polluting solution's amount (L), *W* – Indicates the mass of the used beads (g).

Table 1. The parameters used in these experiments

Parameter	Rang
PH	3,5,7,9,11
Contact time (s)	30,60,90,120,150
Agitation Speed (rpm)	100,150,200,250
Initial phenol Concentration (p.p.m)	50,100,150,200,250
Dose of adsorbent (g)	0.4,0.6, 0.8,1,1.2

Characterization techniques

Several methods were used to characterize the materials both before and after activation in order to comprehend surface and structural alterations. FTIR was used to identify the functional groups, SEM to examine the morphology and surface, BET to assess the surface area and porosity, and XRD to analyze the crystalline structure. These methods provide a thorough assessment of how activation affected the material's characteristics. All batch adsorption experiments were conducted in triplicate under controlled laboratory conditions, and the average values were reported. Experimental parameters were varied individually while keeping the remaining parameters constant to accurately evaluate the influence of each operational factor on phenol adsorption. The experimental error was maintained within ±5%.

Study samples and their collection

Prior to treatment, the adsorbents were analyzed on industrial water samples from the Daura refinery in Baghdad, and the concentration of phenol in these samples was measured beforehand as well as after the adsorbent was added. Phenol analysis was performed using a spectrophotometer with a commercial Merck reagent kit following the manufacturer's procedure. Predosed reagents and factory-prepared calibration standards supplied with the kit were used for the colorimetric determination of phenol concentration.

RESULTS AND DISCUSSION

Adsorbent characteristics

FTIR test

The FTIR spectra shown in Figure 3 represent the times before, after, and three times after phenol adsorption. The large peaks at 3424 cm^{-1} (both before and after activation) are caused by vibrations of stretching of hydroxyl surface structures, absorbed water, and OH stretch of alcohols contained in the lignocellulosic matrix. Nevertheless, after adsorption, this absorbed band will blend in with the sample's adsorbed phenolic hydroxyl groups. The sample's OH group peak intensity is lower after adsorption, than prior to activation; however, this peak's strength increases following phenol adsorption. The strong peaks at about 1635 cm^{-1} may be caused by C=C bonds. Since phenol structures contain the c=c aromatic double bond, the strength of this peak rises as phenol groups are adsorbed. The carbonyl group of esters is linked to the peak at 1744 cm^{-1}. The twin peaks at roughly 2922.0 and 2852.0 cm^{-1} in the before activation sample (B3) may indicate the CH stretching (asymmetric and symmetric stretches) of the CH2 and CH3 groups, as well as their bending vibration at about 1469.0 cm^{-1}. During activation, sharper peaks at 1103 were seen compared to previously, indicating a rise in functional groups with single oxygen bonds, particularly in the COC group (phenols, esters, lactones, ethers, and alcohols). Methyl rock (13821/cm) and CH scissoring (1468 cm^{-1}) are matched at 1387 1/cm and 1469 1/cm, respectively. After activation and adsorption, the intensity of the OH peak decreases, suggesting that some elements of the base material have benefited from activation**.**

Scanning electron microscopy (SEM)

The pre- activation SEM micrographs show that the material is made up of large, asymmetrical agglomerates with extremely low surface pores and level of roughness, as shown in Figure 4(a). The particles seem to be poorly dispersed and form agglomerates that mask the surface area available. However, at higher magnification, the average particle size measured was 64.25 nm, indicating that even though the nanostructure is fairly coarse and not extensively exposed, as shown in Figure 4(c). Such morphological features indicate poor reactivity, possibly owing to the limited surface area and restricted active sites.

Upon activation, a drastic morphological change is evident in SEM images. As seen in Figure 4(b), the surface is considerably rougher and more porous, with a shift to thinner and evenly distributed nanoparticles. The particle size has significantly decreased to about 22.670 nm in the high magnification photograph.

Brunauer–Emmett–Teller (BET)

It showed a good increase in surface area from 2.1078 m^2/g prior to activation, up to 1087 m^2/g following the activation process. In order to increase the adsorption efficiency of the material and open its pores, the activation procedure proved to be highly successful. Additionally, the data showed that the pore volume doubled from 0.00305490 cm^3/g to 0.8180 cm^3/g. This is an

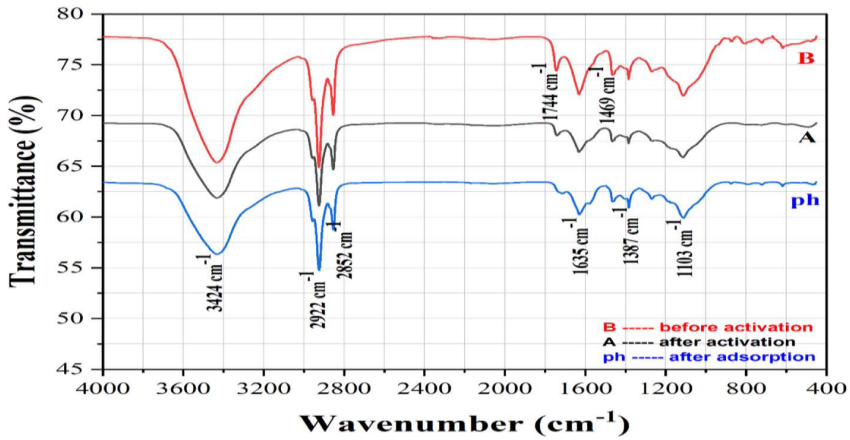

Figure 3. The FTIR spectrum of DK

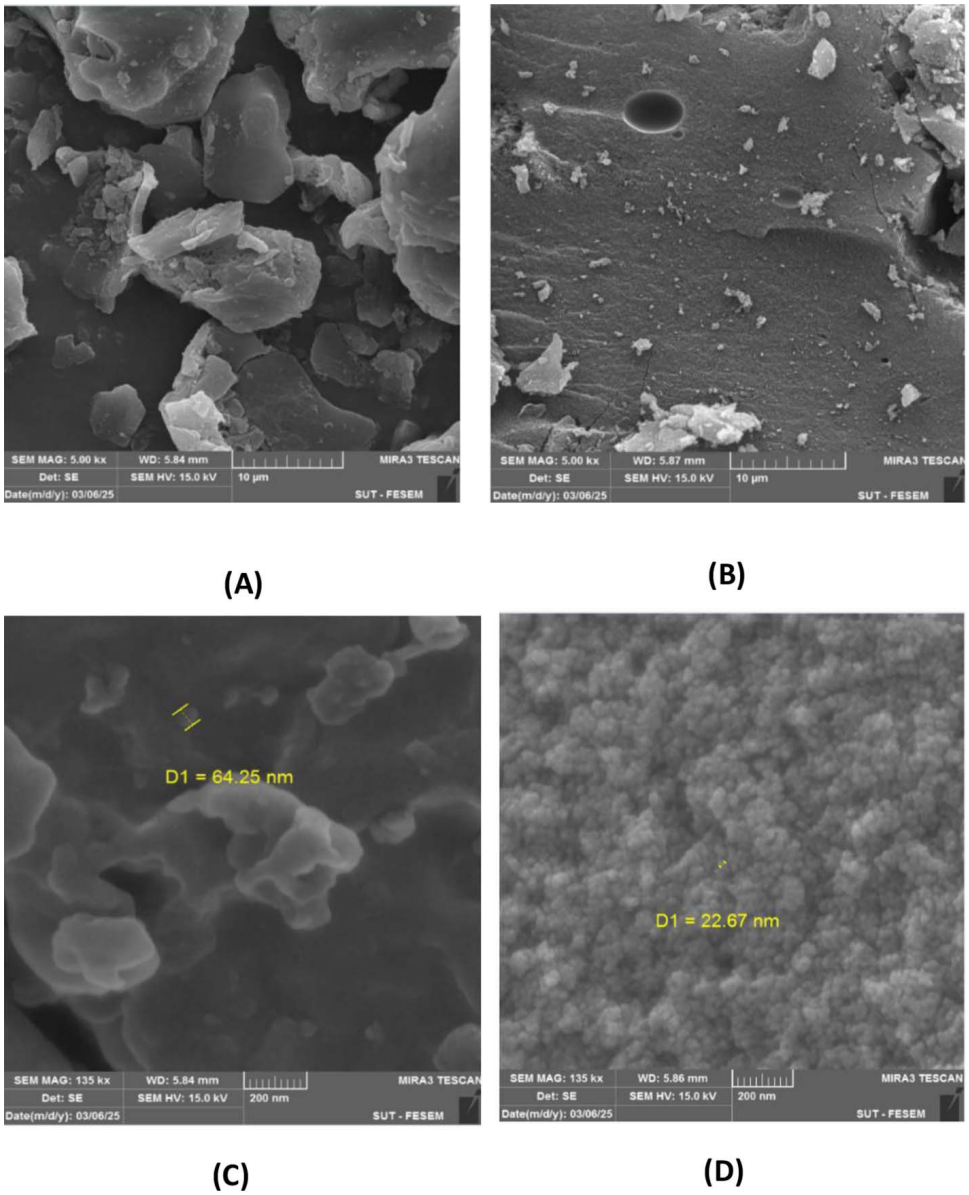

Figure 4. SEM images of date kernels: (a) before activation with rough non-porous surface, (b) after activation showing porous structure, (c) particle size measurement before activation (64.25 nm), (d) particle size measurement after activation (22.67 nm)

important enhancement that indicates the development of a new conventional internal porous architecture within the material upon activation.

As is often seen after biochar activation, the findings also showed that in addition to increased surface area, the average pore size decreased from 5.7971 nm for the untreated biochar to 3.0124 nm, suggesting a structural transformation of mesopores/macropores into micropores. This material is appropriate and beneficial for adsorption, pollutant removal, and storage inside the adsorbate due to the aforementioned improvement in characteristics. Table 2.

Diffraction of X-rays

The pattern of XRD of the crystals appeared before phenol adsorption, with different intensities of peaks at different 2θ angles, indicating the arrangement of the crystalline structure of the material. The peaks correspond to every specific crystal plane and its spacing, which reflect the initial material structure, see Figure 5. The XRD pattern clearly displays variations in peak strength at specific 2θ angles following phenol adsorption (Blue Curve). Indeed, the observed differences indicate that phenol adsorption caused changes in the crystalline structure of the material, either by modifying the distance between crystal planes or affecting its degree of crystallinity. This change in maximum intensity indicates adsorption and possible structural rearrangements or the phase composition. As shown in Figure 5, the comparison between the two patterns clearly reveals the significant effects of phenol adsorption on the crystalline nature and structural modifications of the material due to phenol adsorption.

Phenol elimination using batch adsorption studies

PH levels tested

The results showed that phenol removal efficiency before activation was very low, ranging from 0.26% at pH 11 to 2.28% at pH 3, indicating the limited adsorption capacity of the raw material. After activation, the efficiency increased significantly, ranging from 71.30% to 99.34%, with the highest value at pH 5 and the lowest at pH 11. This remarkable improvement is attributed to the increased porosity and number of active surface sites after activation (Komnitsas and Zaharaki, 2016), in addition to the fact that the slightly acidic medium enhanced the binding of phenol molecules to the adsorbent, see Figure 6.

Table 2. Key findings from the BET analysis for DK

No.	Proprietorship	Before activation	After activation
1	Langmuir area	3.1932 m²/g	914.73 m²/g
2	Total pore volume	0.00305490 cm^3/g	0.8180 cm^3/g
3	Average pore diameter	5.7971 nm	3.0124 nm
4	Surface area (BET)	2.1078 m²/g	1087 m²/g

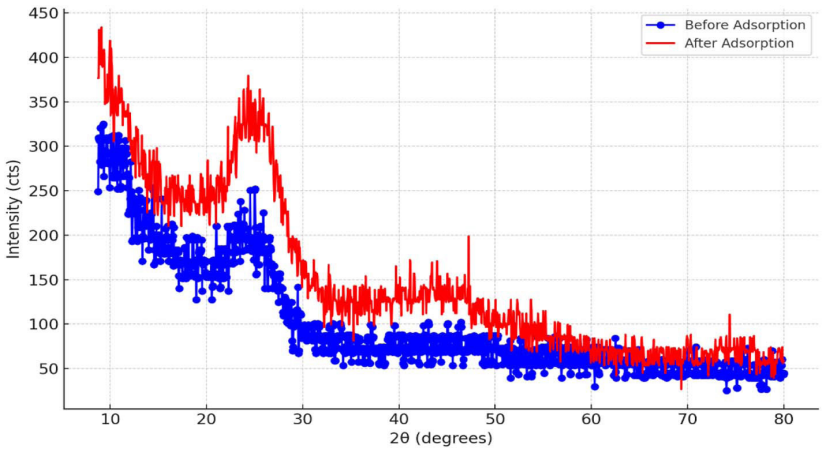

Figure 5. XRD patterns of date kernels before and after phenol adsorption, showing changes in crystalline structure and peak intensities

Contact time

The results showed that phenol removal efficiency before activation was low, ranging from 0.53% at 150 min to 12.53% at 60 min Figure 7, indicating unstable and limited adsorption performance in the raw state. After activation, the efficiency improved substantially, ranging from 69.22% at 30 min to 99.97% at 150 min, with a steady increase over time. This significant improvement reflects the enhanced surface properties and the greater availability of active sites after activation, allowing for more effective and sustained adsorption as the contact time increased (Dhidan, 2023).

Agitation speed

The data show that phenol removal efficiency before activation was very low, ranging from 0.3% at 100 rpm to 2.08% at 150 rpm, indicating poor adsorption in the raw material. After activation, efficiency increased significantly, ranging from 25.44% at 100 rpm to 99.34% at 200 rpm (Díaz et al., 2024), with a slight decrease to 89% at 250 rpm. This suggests that moderate stirring speeds enhance adsorption by improving mass transfer, while very high speeds may reduce contact time between phenol molecules and the adsorbent surface, slightly lowering removal efficiency, see Figure 8.

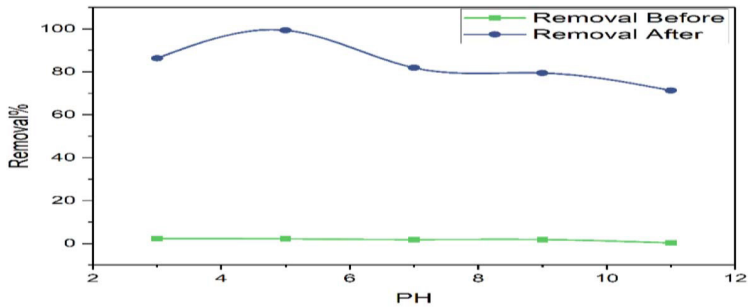

Figure 6. Impact of the acidic activity (pH) on the phenol removal of DK before and after activation at (starting phenol content of 50 mg/l, adsorbent dosage of 0.8 g, contact time of 120 min, speed of 200 rpm)

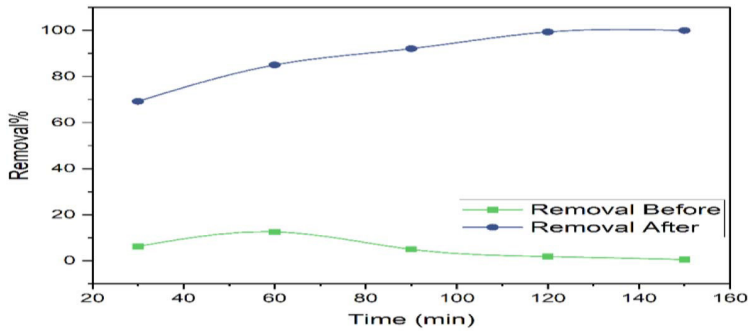

Figure 7. Impact of the contact period on date kernel phenol effective removal, both prior to and after activation process at pH 7.0, adsorbent quantity of 0.80 g, initial phenol concentration of 50 mg/L, and the agitation rate of 200.0 rpm

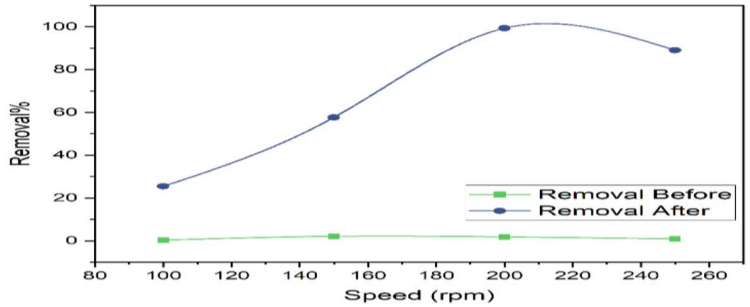

Figure 8. Impact of speed of agitation on date kernel phenol removal effectiveness both prior to and post- activation at starting phenol amount of 50.0 mg/L, dosages of a of 0.80 g, and contact period of 120.0 minutes

Initial phenol concentration

The phenol removal efficiencies before activation were extremely low: 1.68% at an initial concentration of 250 mg/L and 2.75% at an initial concentration of 150 mg/L, indicating low adsorption capacity of the raw material (Ghanadzadeh Gilani et al., 2019). Once activated, the efficiency increased significantly from 71.75% to 99.74%, with the greatest values recorded at a concentration of phenol ranging from 50 mg/L to 150 mg/l; although there was a slight decline at the higher concentrations (200–250 mg/l) due to enriched active sites on surfaces of adsorbent being reached, making binding to other phenol molecules less efficient, as seen in Figure 9.

Dosage of adsorbent

The low phenol removal efficiency in the unactivated condition, from 1.53% at a dose of 0.4 g to 4.46% at a dose of 1.2 g (A), indicates weak adsorption properties for the raw material. After activation, the efficiency increased significantly (73.56%–99.80%) (Figure 10), with the values gradually increasing from a dosage of 0.8 g to achieve the highest value with doses of 0.8 g or more. This significant enhancement is attributed to increased porosity and the number of active surface sites, in addition to the effect of higher doses in providing a larger surface area for phenol molecule adsorption (Ghanadzadeh Gilani et al., 2019).

Adsorption isotherm models

Different fit behaviors to experimental data were observed in the four adsorption models for phenol adsorption onto DK material, see Table 3. The Langmuir model had the best coefficient of determination values (William Kajjumba et al., 2019), demonstrating a high accuracy of data fitting and indicating that the adsorption occurs on a didactic surface, covering through monolayer mechanics. Following this, the Dubinin–Radushkevich (D–R) model was applied to predict and describe the adsorption behavior with high accuracy, while also providing information

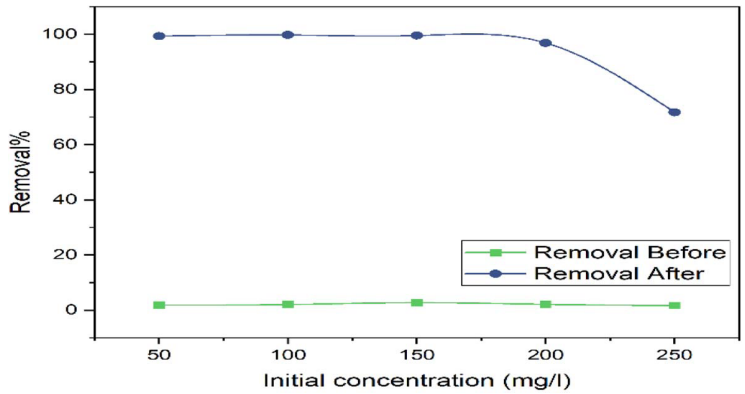

Figure 9. Impact of starting phenol concentration on date kernel removal effectiveness both before and following activation at pH 7.0, adsorbent concentration of 0.80 g, contact period of 120.0 minutes, and agitation rate at 200.0 rpm

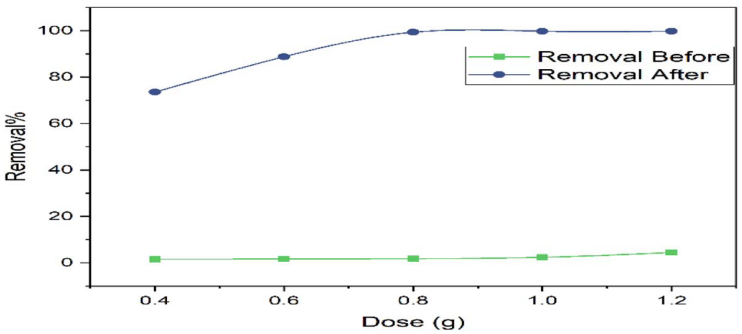

Figure 10. Impact of adsorbent dosage on date kernel phenol removal efficiency both prior to and after activation at pH 7, starting phenol amount of 50.0 mg/L, contact period of 120.0 minutes, and agitation rate of 200.0 rpm

about the type of process; energy calculations found from this model supported an energy lower than 8 kJ/mol, which confirms that the mechanism is non-chemical in nature, as it follows van der Waals forces. The Temkin model provided a reasonable fit, considering the energy changes and interaction between adsorbed molecules. On the other hand, the Freundlich model was the least conformed to data corresponding to a heterogeneous surface, although it can have some applicability to this material in terms of phenol adsorption. In general, it means that the Langmuir model is the best in describing the adsorption process for this material, the D–R model is in the second position for this material, while for the other two last positions are the Temkin and the Freundlich models, see Figure 11.

Kinetic models analysis

The kinetics of phenol adsorption onto DK material were tested using first-order, second-order, and intraparticle diffusion models. The second-order kinetic model had the highest correlation coefficient (R^2 = 0.999), indicating that the adsorption follows a second-order mechanism, which is characteristic of a chemisorption type process and operates via valence forces through the sharing or exchange of electrons between the adsorbent and adsorbate. In comparison, the first-order model exhibited a low fit (R^2=0.3914), indicating that the first-order kinetics cannot sufficiently describe the adsorption kinetic behavior of this system. The intraparticle diffusion model showed a high

Table 3. Comparison of the adsorption isotherm models for phenol adsorption onto DK material

Model	Linear equation	R^2	Main interpretation
Langmuir (A)	y = 0.0164x + 0.0082	0.9943	Best fit; homogeneous surface; monolayer adsorption
Temkin (B)	y = 6.7035x + 43.383	0.9192	Considers energy changes and adsorbate–adsorbate interactions
Freundlich (C)	y = 0.1629x + 1.6159	0.8412	Heterogeneous surface; less accurate fit
Dubinin–Radushkevich (D)	y = -3×10⁻⁸x + 4.0258	0.9668	Good fit; indicates physical adsorption (E < 8 kJ/mol)

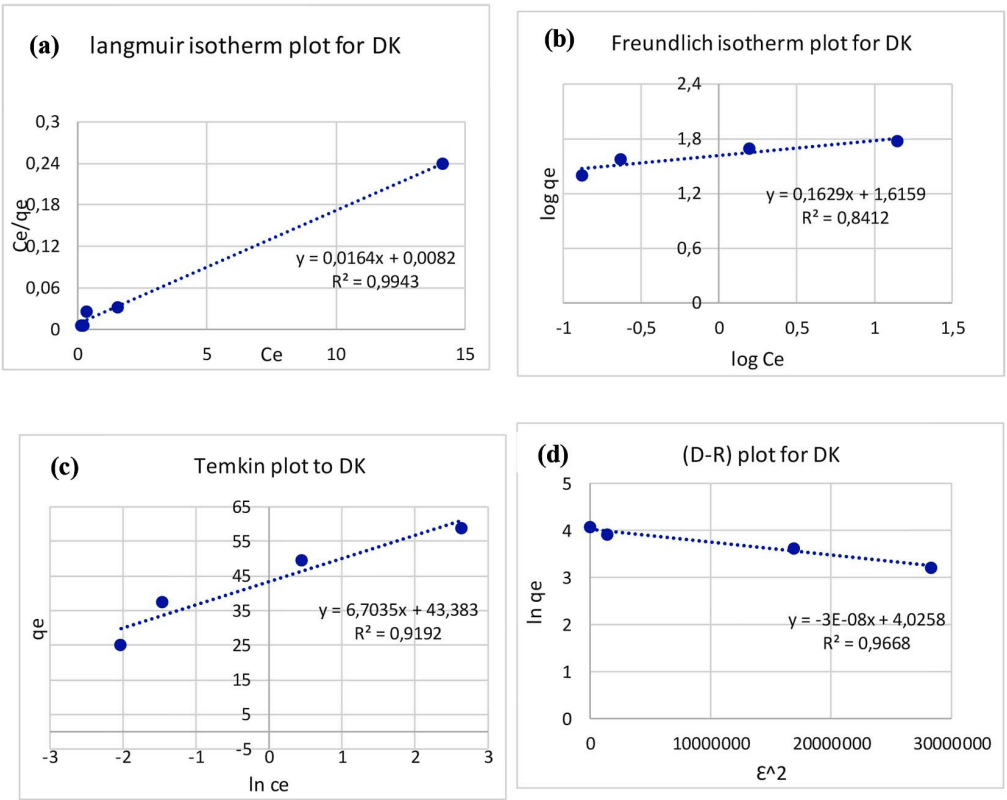

Figure 11. The Langmuir, Freundlich, Temkin, and Dubinin-Radushkevich adsorption isotherm models are used to remove phenol

correlation coefficient (R^2=0.9509), indicating a significant contribution of intraparticle diffusion to the overall adsorption process; meanwhile, the intercept value suggests that this mechanism itself is not the only rate-controlling step and it may be done in conjunction with boundary layer effects. In summary, the results confirm that the adsorption kinetics of phenol onto DK were described by a second-order model followed by an intraparticle diffusion model, whereas the first-order model is poorly suited to this system, see Table 4 and Figure 12.

Results samples of the study

Before treatment, the concentration of phenol in a sample obtained from the AL Dora refinery was tested. The removal efficiency for DK was then determined by testing the products produced under normal conditions and measuring the concentration of phenol following a typical treatment. Table 5 displays the results.

DISCUSSION

The adsorption behavior observed in the present study can be mechanistically attributed to the physicochemical interactions between the molecules of phenol and the active sites available on the synthesized biochar surface. The reasons for such a high removal efficiency are probably due to the large specific surface area and a large number of various surface functional groups, which increase the easy accessibility of adsorption sites. The adsorption process is

Table 4. Comparison of the kinetic models for phenol adsorption onto DK material

Model	Linear equation	R^2	Main interpretation
First-order (A)	y = -0.0086x + 0.7147	0.3914	Poor fit; does not represent adsorption kinetics well
Second-order (B)	y = 0.0703x + 1.3929	0.999	Best fit; indicates chemisorption mechanism
Intraparticle diffusion (C)	y = 0.5803x + 5.8126	0.9509	Significant contribution from intraparticle diffusion; not the only rate-controlling step

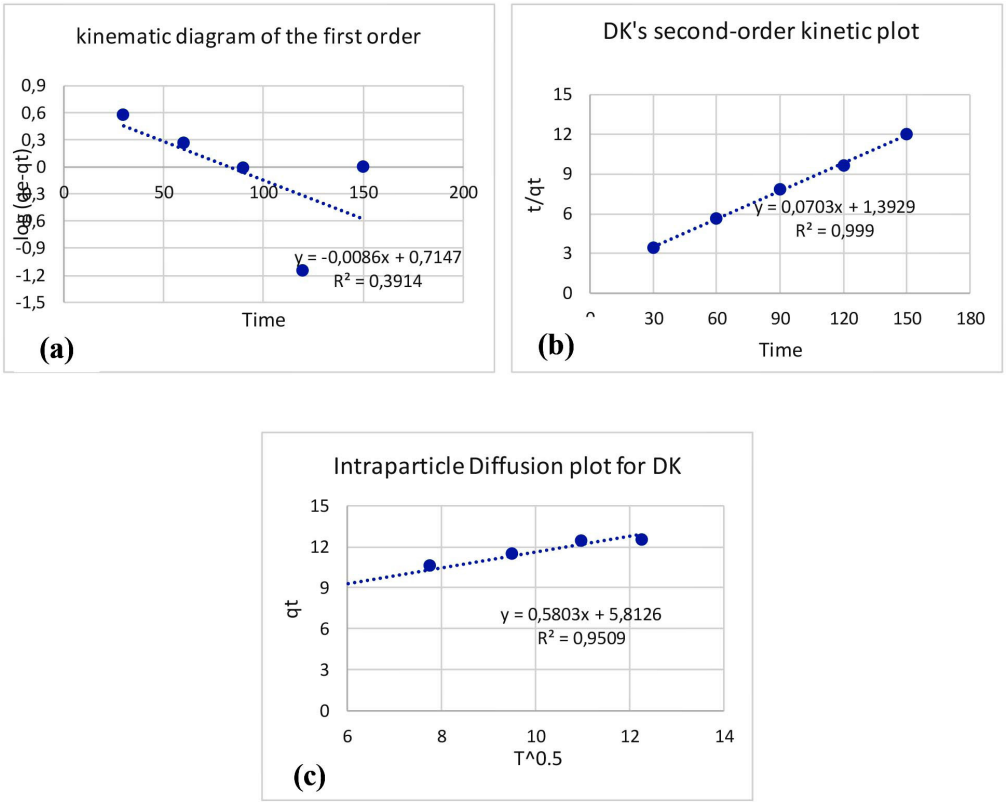

Figure 12. Three kinetic models – the pseudo-first-order model, the pseudo-second-order kinetics model, and the intraparticle diffusion-based model – are applied to phenol adsorption

Table 5. Results obtained before and after treatment with the adsorbent DK

Phenol concentration before treatment	Phenol concentration after treatment	Removal%
10.65 mg/l	1.11 mg/l	89.5774648

Note: PH = 5, Speed = 200 rpm Time = 90 min Dose = 0.8 g.

multifactorial, which can include mechanisms of electrostatic attraction, π–π interactions, hydrogen bonding, and pore-filling effects based on the surface chemistry of the prepared biochar. Moreover, the satisfactory fit of the experimental data with the Langmuir isotherm model indicates that in adsorption, a mostly monolayer coverage on a relatively homogenous active site was shown. Similar adsorption behavior has been reported in previous studies involving nanostructured adsorbents for organic contaminant removal, where nanoscale morphology and surface functionalization played significant roles in improving adsorption capacity and pollutant affinity (Mustapha et al., 2026). Therefore, the obtained results confirm that the prepared nanomaterial possesses favorable surface characteristics for efficient adsorption of organic compounds from aqueous solutions.

CONCLUSIONS

It was shown that the adsorption capacity of phenol by the date kernel biochar was augmented by phosphoric acid activation. The presence of newly formed oxygen-containing functional groups and the creation of well-developed nanostructure, highly porous surface morphology, after the activation procedure were confirmed via FTIR and SEM analyses, respectively. The substantial increment in surface area and pore volume indicated by the BET results validated this, which further correlated with the enhanced adsorption efficacy (over 99% at optimum conditions). The structural changes were evidenced by XRD analysis after phenol adsorption, which suggested strong interactions between phenol molecules and the surface of biochar. Adsorption isotherm studies revealed that the best correlation was observed with the Langmuir model, suggesting monolayer adsorption on a surface that is homogeneous, together with a fit with the Dubinin–Radushkevich model indicating contribution of physical adsorption. Kinetic modeling showed that the process was best fitted by the pseudo-second-order model, confirming that chemisorption is the controlling process in these systems, and that intra-particle diffusion also plays a role in the rate. However, some limitations should also be noted, although the synthesized biochar exhibited excellent adsorption performance for the removal of the studied phenol. The large-scale application may be influenced by factors such as material production cost, regeneration efficiency, structural stability, and long-term operational performance. Future research should also focus on pilot-scale implementation to enhance the practical applicability and industrial scalability of the developed adsorption system. Overall, these results confirm that activated biochar derived from date kernels is a promising, low-cost, and eco-friendly adsorbent with high potential for phenol removal from wastewater.

Acknowledgment

The authors acknowledge the faculty of Engineering, Mustansiriyah University (www.uomustansiriyah.edu.iq), for their valuable support.

REFERENCES

1. Abdullah, S. A., Naser, Z. A. R., Kariem, N. O. (2025). Preparation of eco-friendly activated biochar using peach Kernal as an adsorbent for phenols from waste water. *Al-Rafidain Journal of Engineering Sciences 3*(2).
2. Alfyad, S. A., Kariem, N. O., Naser, Z. A. (2025). Synthesis of eco-friendly activated biochar using mix shells as an adsorbent for phenols from waste water. *Journal of Ecological Engineering*, *26*(10), 166–179. https://doi.org/10.12911/22998993/205798
3. Alhamd, S. J., Abbas, M. N., Jawad Al-Fatlawy, H. J., Ibrahim, T. A., Abbas, Z. N. (2024). Removal of phenol from oilfield produced water using non-conventional adsorbent medium by an eco-friendly approach. *Karbala International Journal of Modern Science*, *10*(2). https://doi.org/10.33640/2405-609X.3350

4. Al-Khalid, T., Surkatti, R., El-Naas, M. H. (2020). Organic Contaminants in Industrial Wastewater: Prospects of Waste Management by Integrated Approaches. In M. Shah & A. Banerjee (Eds.), *Combined Application of Physico-Chemical & Microbiological Processes for Industrial Effluent Treatment Plant* (pp. 205–235). Springer Singapore. https://doi.org/10.1007/978-981-15-0497-6_10
5. Bartolomeu, M., Neves, M. G. P. M. S., Faustino, M. A. F., Almeida, A. (2018). Wastewater chemical contaminants: Remediation by advanced oxidation processes. *Photochemical & Photobiological Sciences*, *17*(11), 1573–1598. https://doi.org/10.1039/c8pp00249e
6. Chen, Q., Zhang, T. C., Ouyang, L., Yuan, S. (2022). Single-step hydrothermal synthesis of biochar from H_3PO_4-Activated lettuce waste for efficient adsorption of Cd(II) in aqueous solution. *Molecules*, *27*(1), 269. https://doi.org/10.3390/molecules27010269
7. Dhidan, S. K. (2023). Removal of phenolic compunds from aqueous solutions by adsoption onto activted carbons prepared from date stones by chemical activation with $FeCl_3$. *Journal of Engineering*, *18*(1), 64–77. https://doi.org/10.31026/j.eng.2012.01.05
8. Díaz, B., Sommer-Márquez, A., Ordoñez, P. E., Bastardo-González, E., Ricaurte, M., Navas-Cárdenas, C. (2024). Synthesis methods, properties, and modifications of biochar-based materials for wastewater treatment: A review. *Resources*, *13*(1), Article 1. https://doi.org/10.3390/resources13010008
9. El-Naas, M. H., Al-Zuhair, S., Alhaija, M. A. (2010). Removal of phenol from petroleum refinery wastewater through adsorption on date-pit activated carbon. *Chemical Engineering Journal*, *162*(3), 997–1005. https://doi.org/10.1016/j.cej.2010.07.007
10. Farzana, M., Marjanul Haque, Md., Sonali, S., Saha, A., Razzak, Md., Amin Khan, R. (2023). Types and treatment technology of industrial wastewater. *Journal of Chemical, Environmental and Biological Engineering*. https://doi.org/10.11648/j.jcebe.20220602.12
11. Ghanadzadeh Gilani, A., Ghanadzadeh, H., Azmoon, P., Chaibakhsh, N. (2019). Phenol adsorption from aqueous phase onto prepared low-cost carbons from natural sources: A comparative study. *Physical Chemistry Research*, *7*(2). https://doi.org/10.22036/pcr.2019.160071.1572
12. Hualpa-Cutipa, E., Acosta, R. A. S., Sangay-Tucto, S., Beingolea, X. G. M., Gutierrez, G. T., Zabarburú, I. N. (2022). Recent trends for treatment of environmental contaminants in wastewater: An integrated valorization of industrial wastewater. In *Integrated Environmental Technologies for Wastewater Treatment and Sustainable Development* (pp. 337–368). Elsevier. https://doi.org/10.1016/B978-0-323-91180-1.00007-7
13. Hussain, O. A., Hathout, A. S., Abdel-Mobdy, Y. E., Rashed, M. M., Abdel Rahim, E. A., Fouzy, A. S. M. (2023). Preparation and characterization of activated carbon from agricultural wastes and their ability to remove chlorpyrifos from water. *Toxicology Reports*, *10*, 146–154. https://doi.org/10.1016/j.toxrep.2023.01.011
14. Kariem, N. O., Sachit, D. E., Ismael, Z. Q. (2018). The performance of a spiral wound RO membrane to desalinate a brackish groundwater in the middle of Iraq. *Desalination and Water Treatment*, *136*, 72–82. https://doi.org/10.5004/dwt.2018.23097
15. Komnitsas, K. A., Zaharaki, D. (2016). Morphology of modified biochar and its potential for phenol removal from aqueous solutions. *Frontiers in Environmental Science*, *4*. https://doi.org/10.3389/fenvs.2016.00026
16. Kumar, N. S., Shaikh, H. M., Asif, M., Al-Ghurabi, E. H. (2021). Engineered biochar from wood apple shell waste for high-efficient removal of toxic phenolic compounds in wastewater. *Scientific Reports*, *11*(1), 2586. https://doi.org/10.1038/s41598-021-82277-2
17. Manasa, R. L., Mehta, A. (2020). Wastewater: Sources of Pollutants and Its Remediation. In K. M. Gothandam, S. Ranjan, N. Dasgupta, E. Lichtfouse (Eds.), *Environmental Biotechnology 2* (Vol. 45, pp. 197–219). Springer International Publishing. https://doi.org/10.1007/978-3-030-38196-7_9
18. Mohamad Said, K. A., Ismail, A. F., Abdul Karim, Z., Abdullah, M. S., Hafeez, A. (2021). A review of technologies for the phenolic compounds recovery and phenol removal from wastewater. *Process Safety and Environmental Protection*, *151*, 257–289. https://doi.org/10.1016/j.psep.2021.05.015
19. Mustapha, S. I., Muritala, K. B., Oguntuase, A. A., Adewoye, T. L., Isa, Y. M. (2026). Phenol removal from wastewater using biochar-based composites. In *Wastewater Treatment with Biochar* (pp. 365–381). Elsevier. https://doi.org/10.1016/B978-0-443-29865-3.00017-0
20. Nasir, M., Kadhum, Z., Kariem, N., Jasim, Z. (2022). Removal of sesame oil from artificial wastewater applying Fenton process and comparing it with actual wastewater. *Journal of Ecological Engineering*, *23*(10), 248–254. https://doi.org/10.12911/22998993/152518
21. Nguyen, N.-T., Lin, A., Chang, C.-T., Hong, G.-B. (2025). Bimetallic zinc-iron-modified sugarcane bagasse biochar for simultaneous adsorption of arsenic and oxytetracycline from wastewater. *Molecules*, *30*(3), 572–572. https://doi.org/10.3390/molecules30030572

22. Önal, Y., Küçük, İ. (2020). Low cost activated carbon synthesis, characterization and adsorption applications. *NATURENGS MTU Journal of Engineering and Natural Sciences, Malatya Turgut Ozal University*, *1*(2), 32–38. https://doi.org/10.46572/nat.2020.14
23. Saravanan, A., Senthil Kumar, P., Jeevanantham, S., Karishma, S., Tajsabreen, B., Yaashikaa, P. R., Reshma, B. (2021). Effective water/wastewater treatment methodologies for toxic pollutants removal: Processes and applications towards sustainable development. *Chemosphere*, *280*, 130595. https://doi.org/10.1016/j.chemosphere.2021.130595
24. William Kajjumba, G., Emik, S., Öngen, A., Kurtulus Özcan, H., Aydın, S. (2019). Modelling of Adsorption Kinetic Processes—Errors, Theory and Application. In S. Edebali (Ed.), *Advanced Sorption Process Applications*. IntechOpen. https://doi.org/10.5772/intechopen.80495
25. Yang, R., Jia, A., He, S., Hu, Q., Sun, M., Dong, T., Hou, Y., Zhou, S. (2021). Experimental investigation of water vapor adsorption isotherm on gas-producing Longmaxi shale: Mathematical modeling and implication for water distribution in shale reservoirs. *Chemical Engineering Journal*, *406*, 125982. https://doi.org/10.1016/j.cej.2020.125982